46th Annual Review of Progress in Quantitative Nondestructive Evaluation
QNDE2019
July 14-19, 2019, Portland, OR, USA

QNDE2019-6832

INDUCTION INFRARED THERMOGRAPHY FOR NON-DESTRUCTIVE EVALUATION OF ALLOY SENSITIZATION

Matthew Roberts, Kevin Wang
Virginia Polytechnic Institute and State University
Blacksburg, VA

Emily Guzas[1]
Naval Undersea Warfare Center
Newport, RI

ABSTRACT

We investigate the efficacy of using induction infrared thermography (IIRT) to detect sensitization in chromium steel. Sensitization refers to the precipitation of certain compounds — $Cr_{23}C_6$ in chromium-steel — at grain boundaries due to cyclic temperature variations, which makes the alloy susceptible to corrosion, environmentally assisted cracking (EAC), and broader failure. In this talk, we first present an experimental study to demonstrate the feasibility of the method. We use welding to induce sensitization in chromium-steel specimens (in the heat-affected zones (HAZ) adjacent to the weld) and conduct IIRT testing using an inductor wand and a FLIR SC8203 infrared camera. Next, we present a computational study to simulate the experiment and compare with the experimental results. Specifically, we present a thermo-electro-magnetic model including Fourier's law of heat conduction and Maxwell's equations for predicting the electromagnetic field caused by a sinusoidal excitation current through the inductor coil. We also introduce an empirical model to relate the density and thickness of sensitized grain boundaries with the local increase in eddy current density which are solved using the commercially available software COMSOL. Finally, we compare the experimental and computational results and discuss the capability of the proposed IIRT method for detecting sensitization in chromium steels.

Keywords: induction infrared thermography (IIRT), sensitization, corrosion, numerical simulation

1. INTRODUCTION

The sensitization of stainless steels is a well-understood problem that affects an array of high-carbon alloys in a range of industries. This phenomenon describes the process by which a steel sample or component has its temperature raised (either naturally or artificially) above a critical threshold (in excess of ~1000° F [1]) for a specific length of time followed by a cooling period. It is through this heating and cooling cycle that chromium carbides ($Cr_{23}C_6$) precipitate at the material's natural grain boundaries (Figure 1). With chromium being a primary contributor to a stainless steel's corrosion-inhibiting properties, the formation of these carbides depletes the grain boundaries of these benefits and leaves these regions susceptible to intergranular corrosion (IGC), environmentally-assisted cracking (EAC), and broader failure.

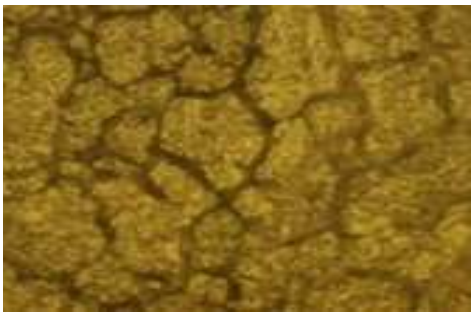

FIGURE 1: MICROGRAPH OF SENSITIZED 440C STEEL, SHOWING THICKENED GRAIN BOUNDARIES.

Current methods for sensitization detection (e.g. ASTM A262-15 for austenitic stainless steels) require destructive tests in a laboratory environment. Given the extensive use of these high-carbon alloys in a range of industries, a comprehensive, non-destructive method for sensitization detection is desirable. The idea of using IIRT as a non-destructive, *in situ* method is based on the hypothesis that, because the sensitized grain boundaries have a higher electrical resistivity than the original, non-sensitized grain structure, the induced eddy currents are forced to take altered paths through the sensitized material – this would indicate that materials of various degrees of sensitization (DoS) will produce different heat signatures. In particular, it is expected that an infrared (IR) camera could detect the local increase in temperature in sensitized regions without explicitly

[1] Contact author: emily.guzas@navy.mil

resolving the grain boundaries. In this talk, we present a combined experimental and computational study to demonstrate and assess this approach in the context of detecting welding-induced sensitization in the heat affected zones (HAZ) of 440C steel specimens (Figure 2).

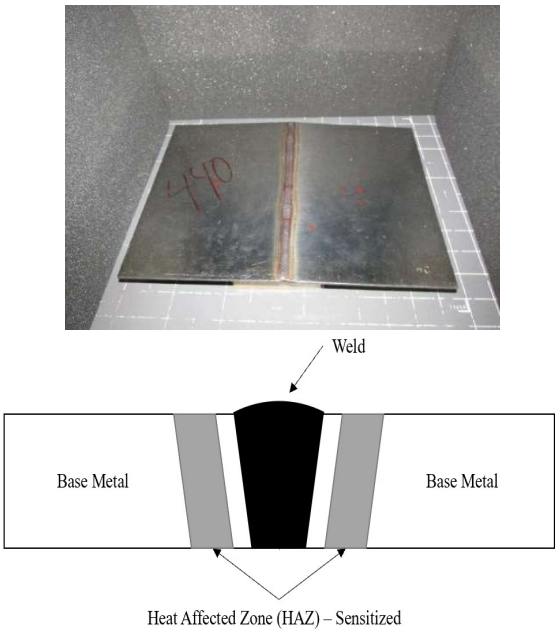

FIGURE 2: A WELDED 440C STEEL PLATE (TOP) AND A SCHEMATIC DRAWING OF WELD AND HAZ REGIONS (BOTTOM).

2. MATERIALS AND METHODS

2.1 IIRT Experiment

We have conducted a series of IIRT experiments at the Naval Undersea Warfare Center, Division Newport (NUWCDIVNPT) in Newport, RI. The typical experimental setup is shown in Figure 3.

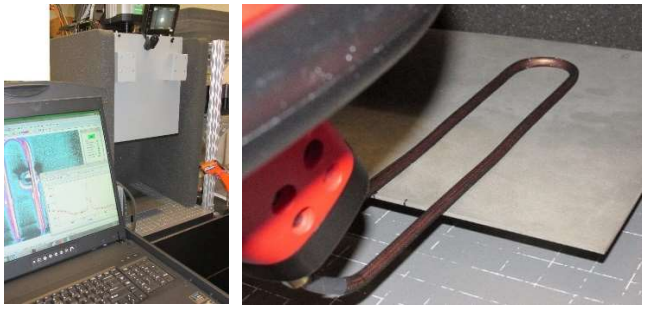

FIGURE 3: EXPERIMENTAL SETUP OF IIRT SENSITIZATION DETECTION.

The experiments included two main goals: (1) draw a correlation between the analog intensity counts that were received by the overhead infrared camera and processed in Thermal Wave Imaging Inc.'s Software, Virtuoso, with a measured increase in temperature due to induction heating, and (2) collect calibration and validation data to be used for comparison to numerical simulations of a developed thermo-electro-magnetic model to describe the induction IRT process through potentially sensitized stainless steel specimens. As previously theorized and demonstrated by Tucker et al. [2], stainless steel specimen regions that possess sensitized material will show a disproportionate increase in intensity (measured by an IR camera) as compared to unsensitized regions of the same material. Developing a model-to-experiment correlation would allow for a wide-range of interpretation to be performed, aided by validated simulations of the physics-based model of the IIRT process for sensitized stainless steels.

The main steps of a typical experiment are as follows:

(1). A metal sample is placed on the table underneath the camera and supported by small cardboard boxes to decouple the heating from the table.
(2). The FLIR infrared camera is brought in to focus above the sample to ensure that the images and data taken were free of distortions and aberrations.
(3). A background thermal scan is performed in conjunction with a temperature reading with an infrared thermometer to relate the radiation seen by the camera with a steady-state temperature.
(4). An electromagnetic coil (e.g., a hairpin-shaped coil as shown in Figure 3) is placed above the sample of interest and energized with an external power supply.
(5). This excitation is performed for a designated period (on the order of seconds) with the coil held in a fixed location before being removed.
(6). After heating, a final temperature is taken with the infrared thermometer in the same position as the baseline reading.

2.2 Modeling and Simulation

The primary equations governing induction originate from the magnetic vector potential formulation of the electromagnetic diffusion equation derived from Maxwell's equations:

$$i\omega\sigma\boldsymbol{A} - \frac{1}{\mu}\nabla^2\boldsymbol{A} = \boldsymbol{J}_S$$

Here, $\boldsymbol{A}$ denotes the magnetic field, $\boldsymbol{J}_S$ the current density of the induction source, ω the angular frequency. μ and σ denotes magnetic permeability and electrical conductivity, respectively. i is the imaginary unit.

Once the eddy currents are induced within a sample, the resultant bulk heating generated by induction is represented by:

$$q_{ind} = \frac{1}{\sigma}|\boldsymbol{J}|^2$$

This induced heat is then used as the source term in Fourier's law of heat conduction to describe the conduction through the specimen. The aggregate heat transfer equation is shown below:

$$\rho C_p \frac{\partial T}{\partial t} - \nabla \cdot (k\nabla T) = q_{ind} - q_{conv} - q_{rad}$$

Here, ρ is the density of the material, T is the temperature, k the thermal conductivity, and C_p the specific heat. q_{conf} and q_{rad}

represent, respectively, the heat losses due to convection and radiation, which are functions of T and the ambient temperature T_∞. The aggregate heat transfer equation is solved in the time domain to find the temperature at a given time and location in the specimen.

COMSOL Multiphysics 5.3a and its AC/DC Module [3] were employed to create and numerically solve the induction heating problem. Per the experimentation performed at NUWCDIVNPT, the model parameters for the 440C plate and the HAZ regions were directly entered into the model. Regarding the coil and the air, the COMSOL-provided values were used with the only adjustment made to the air's conductivity.

The thickness of the plate was exactly matched to that in the experiments, or t=0.125 in (3.2 mm) but other dimensions were approximated. As the critical heating of the plate occurs in a region sufficiently far from the plate edges (in the middle, underneath the coil), there was no need to explicitly model the outermost plate edges in COMSOL. Figure 4 presents the simulation model which includes the sample plate, a hairpin-shaped inductor coil, and the surrounding air.

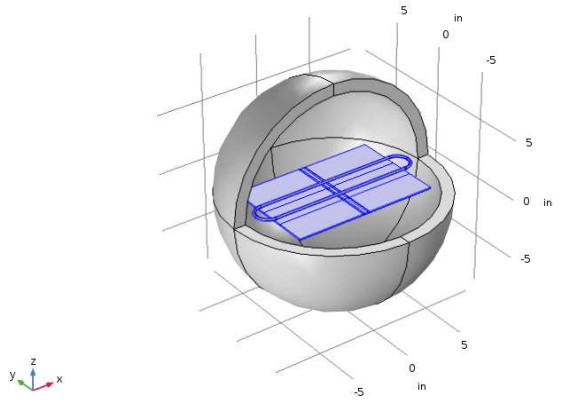

FIGURE 4: COMSOL SIMULATION MODEL, WITH PART OF AIR DOMAIN REMOVED FOR CLARITY.

3. RESULTS AND DISCUSSION

Figure 5 shows the temperature measurement of sensitized 440C steel obtained from the IIRT experiment. Each data series represents the heating (over time) of one point on the surface of the plate. Most of the points are selected within the HAZ regions but there are four distinct points (curves) that heat more slowly than the rest, with the corresponding history points physically located within the weld region.

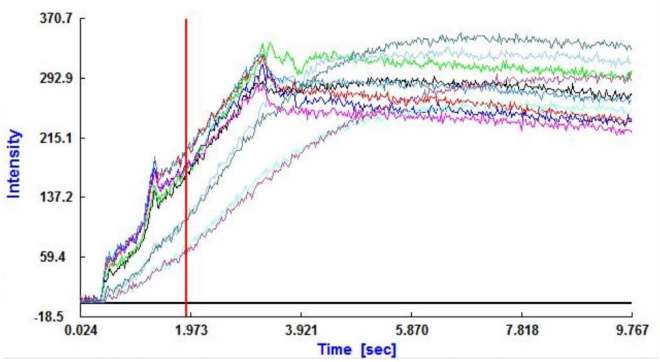

FIGURE 5: IIRT EXPERIMENTAL RESULT: MEASURED INTENSITY VERSUS TIME, AT VARIOUS POINTS ON THE SPECIMEN.

Figure 6 presents a time snapshot of the tempreature field from the COMSOL simulation. Figure 7 superimposes the experimental and simulation result of temperature through a line segment that spans the weld and HAZ regions. In both the experimental and the simulation results, the increase of temperature within the sensitized HAZ regions (adjacent to the weldon either side) is clearly evident.

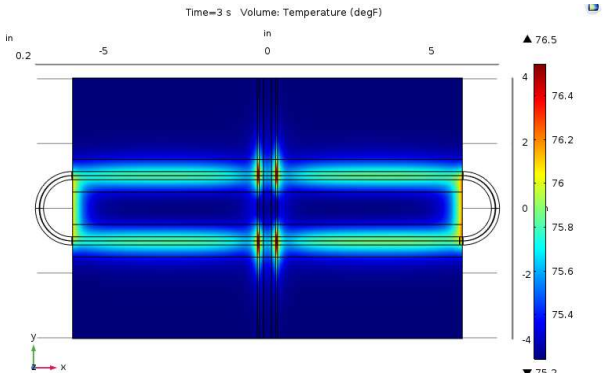

FIGURE 6: COMSOL SIMULATION RESULT

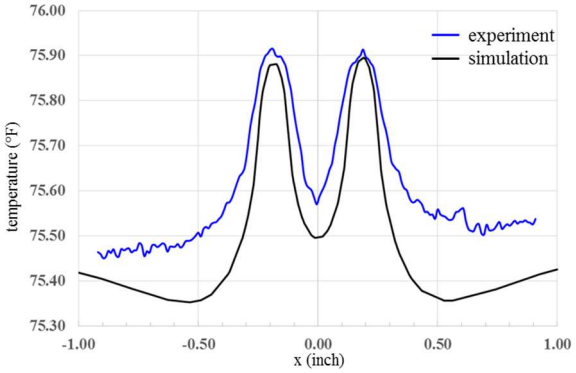

FIGURE 7: COMPARISON OF EXPERIMENTAL AND NUMERICAL RESULTS.

ACKNOWLEDGEMENTS

M.R. and K.W. acknowledge the support of the Office of Naval Research (ONR) through award N00014-18-1-2059. M.R. acknowledges the internship provided by ONR's Naval Research Enterprise Intern Program (NREIP). E.G. acknowledges the support of the Office of Naval Research (ONR) through the Navy Undersea Research Program (NURP), in addition to Wayne Tucker and Patric Lockhart at NUWCDIVNPT for access to experimental facilities, samples, and data.

REFERENCES

[1] C.S. Tedmon Jr., D.A. Vermilyea, and J.H. Rosolowski, "Intergranular corrosion of austenitic stainless steel," *Journal of the Electrochemical Society*, vol. 118, no. 2, pp. 192-202, Feb. 1971.

[2] W.C. Tucker, P. Lockhart, E. Guzas, "Evaluating Sensitized Chromium Steel Alloys with Induction Infrared Thermography," *Journal of Nondestructive Evaluation*, June 2019, 38:42.

[3] COMSOL, Inc. Technical Staff, *AC/DC Module 5.3a User's Guide*, COMSOL Inc., Burlington, MA, 2017.